

P2RX7 plays a critical role in extracellular vesicle-mediated secretion of pathogenic molecules from microglia and astrocytes

Mohammad Abdullah¹ | Zhi Ruan¹ | Seiko Ikezu¹ | Tsuneya Ikezu^{1,2} 

¹Department of Neuroscience, Mayo Clinic Florida, Jacksonville, Florida, USA

²Regenerative Science Graduate Program, Mayo Clinic College of Medicine and Science, Jacksonville, Florida, USA

Correspondence

Tsuneya Ikezu, Department of Neuroscience, Mayo Clinic Florida, Jacksonville, FL 32224, USA.
Email: Ikezu.Tsuneya@mayo.edu

Funding information

National Institute on Aging, Grant/Award Numbers: R01 AG054672, R01 AG066429, R01 AG067763, R01 AG072719, R01 AG079859, RF1 AG054199, RF1 AG082704; Cure Alzheimer's Fund, Grant/Award Number: N/A

Abstract

Extracellular vesicle (EV) secretion is mediated by purinergic receptor P2X₇ (P2RX7), an ATP-gated cation channel highly expressed in microglia. We have previously shown that administration of GSK1482160, a P2RX7 selective inhibitor, suppresses EV secretion from murine microglia and prevents tauopathy development, leading to the recovery of the hippocampal function in PS19 mice, expressing P301S tau mutant. It is yet unknown, however, whether the effect of GSK1482160 on EV secretion from glial cells is specifically regulated through P2RX7. Here we tested GSK1482160 on primary microglia and astrocytes isolated from C57BL/6 (WT) and *P2rx7*^{-/-} mice and evaluated their EV secretion and phagocytotic activity of aggregated human tau (hTau) under ATP stimulation. GSK1482160 treatment and deletion of *P2rx7* significantly reduced secretion of small and large EVs in microglia and astrocytes in both ATP stimulated or unstimulated condition as determined by nanoparticle tracking analysis, CD9 ELISA and immunoblotting of Tsg101 and Flotilin 1 using isolated EVs. GSK1482160 treatment had no effect on EV secretion from *P2rx7*^{-/-} microglia while we observed significant reduction in the secretion of small EVs from *P2rx7*^{-/-} astrocytes, suggesting its specific targeting of P2RX7 in EV secretion except small EV secretion from astrocytes. Finally, deletion of *P2rx7* suppressed IL-1 β secretion and phagocytosed misfolded tau from both microglia and astrocytes. Together, these findings show that GSK1482160 suppresses EV secretion from microglia and astrocytes in P2RX7-dependence manner, and P2RX7 critically regulates secretion of IL-1 β and misfolded hTau, demonstrating as the viable target of suppressing EV-mediated neuroinflammation and tau propagation.

KEYWORDS

astrocytes, ATP, CD9, extracellular vesicle, flotillin-1, GSK1482160, microglia, P2RX7, Tsg101

1 | INTRODUCTION

Microglia are the primary innate immune cells in the central nervous system and play an important role for the homeostatic and protective response to the environment. Extracellular aggregates of amyloid (A β) peptides and neurofibrillary tangles composed of intraneuronal aggregations of hyperphosphorylated microtubule-associate protein tau are a diagnostic hallmark of Alzheimer's disease (AD), the most common form of senile dementia (Brier et al., 2016; Lebouvier et al., 2017). The classification of tau pathology indicates consistent spatiotemporal pattern of disease spread from entorhinal cortex to hippocampal region and cortical area (Braak & Braak, 1991) although the exact mechanism of tau spread contributing to AD progression is not fully understood. We previously reported that microglia secrete extracellular vesicles (EVs), and inhibition of EV synthesis or depletion of microglia

This is an open access article under the terms of the [Creative Commons Attribution-NonCommercial-NoDerivs License](https://creativecommons.org/licenses/by-nc-nd/4.0/), which permits use and distribution in any medium, provided the original work is properly cited, the use is non-commercial and no modifications or adaptations are made.

© 2024 The Author(s). *Journal of Extracellular Biology* published by Wiley Periodicals LLC on behalf of International Society for Extracellular Vesicles.

significantly reduce tau propagation in mouse brains (Asai et al., 2015). We further showed that intrahippocampal injection of EVs collected from tau-phagocytosed murine microglia to the recipient mice can spread tau pathology (Asai et al., 2015). This result was recently validated by our study showing that the inoculation of human AD brain derived EVs highly enriched with pathological tau could propagate tau pathology compared to fibrillar or oligomer form of tau (Ruan et al., 2021), suggesting the pathological role of EV-mediated tau propagation in AD. In addition, Bridging Integrator 1 (BIN1), a late-onset AD risk gene, is critical in microglia-mediated spread of tau pathology via small EV secretion (Crotti et al., 2019). These studies corroborate an idea that EV secretion from microglia is a viable therapeutic target for ameliorating the disease progression.

In this context, we focused on P2X purinoceptor 7 (P2RX7), an ATP-evoked $\text{Na}^+/\text{Ca}^{2+}$ channel that is highly expressed in microglia and astrocytes. Activation of P2RX7 by ATP robustly increases secretion of EVs by depolarization of plasma membranes. A rare loss-of-function mutation of P2RX7 variant (R307Q) is protective against neuroinflammation in multiple sclerosis (Gu et al., 2015). Deletion of *P2rx7* in animal models of tauopathy can reduce tau accumulation, microglial activation, and production of inflammatory molecules, which was accompanied by restoration of synaptic plasticity and memory (Carvalho et al., 2021). These reports indicate that deletion of P2RX7 can suppress tauopathy-related disease progression and neuroinflammation. We have recently shown that administering GSK1482160, an orally applicable CNS-penetrant P2RX7 specific inhibitor, to PS19 mice expressing P301S tau mutant decreased EV secretion from microglia, suppressed tau accumulation in the hippocampal region, and restored memory function (Ruan et al., 2020). P2RX7, however, has not been conclusively tested for its role on EV secretion by comparison of wild type against P2RX7 deficient cell models. Our goal is to determine whether P2RX7 is critical for EV secretion from murine microglia and astrocytes. For that purpose, we tested primary astrocytes and microglia isolated from WT and *P2rx7*^{-/-} pups for ATP-induced EV secretion in the presence or absence of GSK1482160. Our data show that P2RX7 is indeed largely responsible for ATP-induced EV secretion from microglia and astrocytes, the target of GSK1482160, and responsible for EV-mediated secretion of interleukin-1 β and tau.

2 | MATERIALS AND METHODS

2.1 | Reagents

GSK1482160 (334.7236 g/mol, >97% purity, PharmaBlock Sciences, Inc., CAS 1001389-72-5) was diluted in dimethyl sulfoxide (DMSO) as a stock solution to a final concentration of 100 mM. Doses of 50 and 100 μM were used on the astrocyte cells for dose level optimization of GSK1482160. Finally, GSK1482160 was added to the culture medium until it reached a final concentration of 50 μM , either in the presence or absence of 5 mM ATP stimulation, or control vehicle (Ruan et al., 2020).

2.2 | Animals and tissue cultures

All tests were carried out in compliance with the Mayo Clinic Institutional Animal Care and Use Committee's Guidelines for animal experiments. On the first postnatal day, primary murine astrocytes were extracted from the brains of P0-P1 *P2rx7*^{-/-} and WT (C57BL/6) mouse pups as previously reported (Abdullah et al., 2016; Gong et al., 2002). In brief, isolated cortices were minced and the cortical fragments were incubated in 0.25% trypsin and 20 $\mu\text{g}/\text{ml}$ DNase I in phosphate-buffered saline (PBS, 8.1 mM Na_2HPO_4 , 1.5 mM KH_2PO_4 , 137 mM NaCl and 2.7 mM KCl, pH 7.4) at 37°C for 15 min. The fragments were then dissociated into single cells by pipetting, and then the cells were cultured for 10 days on 75- cm^2 flask at a density of 1×10^7 in Dulbecco's modified essential media (DMEM, Invitrogen, 11965118) containing 10% fetal bovine serum (FBS, Invitrogen, 10082147). After 10 days non-astrocytic cells were removed by shaking at 200 rpm for 1 h. Remaining murine astrocytes in the monolayer were trypsinized by 0.1% trypsin-EDTA in PBS and reseeded onto 6 cm^2 dishes. Primary astrocytes were maintained in DMEM containing 10% FBS until use. Primary microglial cultures were prepared from *P2rx7*^{-/-} and C57BL/6 P1 pups as described (Ikezu et al., 2021) using anti-CD11b magnetic beads (Miltenyi Biotec, 130-049-601). Microglia were maintained with DMEM medium with 10% FBS in a 5% CO_2 humidified incubator. Murine monocyte colony stimulating factor M-CSF (10 ng/mL, BioVision, 4238) was added for microglial culture after plating, and every other day. Primary astrocytes and microglia cultured cells were identified through immunocytochemistry using anti-GFAP antibody (Agilent, Z033429-2), S100B (Thermo Fisher Scientific, MA1-25005), and Ibal (Wako, 019-19741).

2.3 | Cell treatment and EV isolation

Prior to collecting conditioned media (CM), microglia and astrocytes were washed twice with double-filtered PBS and replaced with DMEM double-filtered with Millex-HV syringe filter unit 0.45- μm (EMD Millipore, SLHVM33RS) containing a specified concentration of freshly prepared GSK1482160 (PharmaBlock Science, Inc., CAS, 1001389-72-5). Cells were incubated at 37°C

for 1 h, treated with 1 $\mu\text{g}/\text{mL}$ of LPS (Sigma-Aldrich, L3024) for 3 h, followed by stimulation with 5 mM ATP in fresh serum-free media for 15 min for the collection of CM. The CM and cells were collected immediately after the ATP stimulation for further analysis. EVs were isolated from CM by sequential high-speed centrifugation as described (Asai et al., 2015). Briefly, the CM was centrifuged at $300 \times g$ for 10 min, and the supernatant was centrifuged at $2000 \times g$ for 10 min at 4°C to remove cell debris. The supernatant was centrifuged at $10,000 \times g$ for 30 min at 4°C to remove microvesicles. The supernatant was ultracentrifuged at $100,000 \times g$ for 70 min at 4°C to enrich EV fraction in pellets. With our purification method, enriched EVs under ATP stimulation were not positive for apoptotic markers nor contaminated by intracellular organelles derived from damaged cells. The EVs-enriched fraction was collected and stored at -80°C until further use.

For the EV associated tau study, purified recombinant 2N3R (Tau-410) and 2N4R (Tau-441) human tau (hTau, 500 $\mu\text{g}/\text{mL}$, rPeptide, T-1002-1 and T-1001-1) was preincubated with 0.3 mg/mL heparin (cat. no. 07980, Stemcell Technologies, Vancouver, Canada) and purified tau filaments from AD brain (Ruan et al., 2021) to be aggregated at 37°C . One hour prior to the incubation with tau aggregates, 30 μM chloroquine (Sigma, C6628) was added to block lysosomal degradation of tau aggregates. Cells were incubated with aggregated hTau (10 $\mu\text{g}/\text{mL}$) at 37°C for 24 h. For the collection of CM, cells were washed twice with PBS, incubated with double-filtered DMEM, stimulated with 1 $\mu\text{g}/\text{mL}$ LPS for 4 h, followed by incubation with 5 mM ATP for 15 min. The cells were washed twice with ice-cold PBS and stored at -80°C for further experiments. EVs were isolated from CM through the sequential centrifuge and ultracentrifugation. The pellet samples were applied to the qEVoriginal Columns (Izon Science) to collect EVs in pooled fraction 7–9 according to the manufacturer's instruction. The pooled fraction was ultracentrifuged at $100,000 \times g$ for 70 min at 4°C , and the pellets fraction was resuspended with 60 μL of ice-cold double-filtered PBS (dfPBS). The isolated EV sample (30 μL , 860 $\mu\text{g}/\text{mL}$) was treated with or without 20 $\mu\text{g}/\text{mL}$ proteinase K (PK, QIAGEN) and 5 mM CaCl_2 in dfPBS for 1 h at 37°C with gentle vortexing every 15 min. The PK was then inhibited by adding 5 mM phenylmethylsulfonyl fluoride (PMSF) for 10 min at room temperature.

2.4 | Nanoparticle tracking analysis (NTA)

NTA was performed with a NanoSight NS300 (Malvern Panalytical), equipped with a sample chamber and an sCMOS camera as previously described (Muraoka et al., 2020). EVs and CM samples were diluted in dfPBS to adjust the particle numbers to the optimal range (20–100 particles/frame). Particle live-imaging settings were set according to the manufacturer's instruction.

2.5 | Immunoblotting

Equal volumes of the isolated EVs were mixed with the sampling buffer consisting of premixed sample buffer (Bio-Rad, Cat # 1610747), 2-mercaptoethanol (Sigma-Aldrich, Cat # M6250) and were analyzed by 12.5% Tris / tricine (Bio-Rad, Cat # 1610732) SDS-PAGE. The separated proteins were electrophoretically transferred onto PVDF membranes (Immobilon, Millipore) using a transfer buffer (0.1 M Tris, 0.192 M glycine, and 20% methanol). The membrane was subjected to total protein staining by SWIFT membrane staining (VWR 89167-886) and the band intensity was quantified by Gel Doc XR+ Imaging System (Bio-Rad). The membranes were then incubated in a blocking solution consisting of 5% powdered milk in TBS-T (10 mM Tris-HCl, pH 8.0, 150 mM NaCl, and 0.1% Tween 20) overnight at 4°C , followed by immunoblotting with the following EVs specific marker mouse anti-Flotilin 1 (BD Transduction Laboratories, 610820) and Tsg101 (C-2, Santa Cruz Biotechnology, SC-7964), CD81 (LifeSpan Bioscience, LS-C350457), microglial marker Tmem119 (Biolegend, 853302), CD11b (Millipore, CBL1313), astrocytic marker EAAT1 (Abcam, ab416), ITGA6 (Novus Biological, NBP-85747) and non-EV marker GM130 (Santa Cruz Biotechnology, SC-53296), and Cytochrome C (Cell Signaling Technology, 11940S). The band intensity was quantified by Gel Doc XR+ Imaging System (Bio-Rad). The band intensity of interest was normalized by the total band intensity on the membrane as determined by the SWIFT membrane staining.

2.6 | CD9 and IL-1 β ELISA

The amount of secreted EVs were quantified by EV specific marker CD9 ELISA according to the manufacturer's instruction (System Bioscience, EXOEL-CD9A-1) using a microplate reader (BioTek Instruments). IL-1 β level was measured using mouse IL-1 β ELISA kit (Abcam, ab197742).

2.7 | Statistical analysis

Immuno-positive bands visualized by Western blot analysis were quantified using the image analysis software ImageJ 1.46r (NIH). Data are presented as the mean \pm SEM of at least three independent experiments. Statistical comparisons of two groups were per-

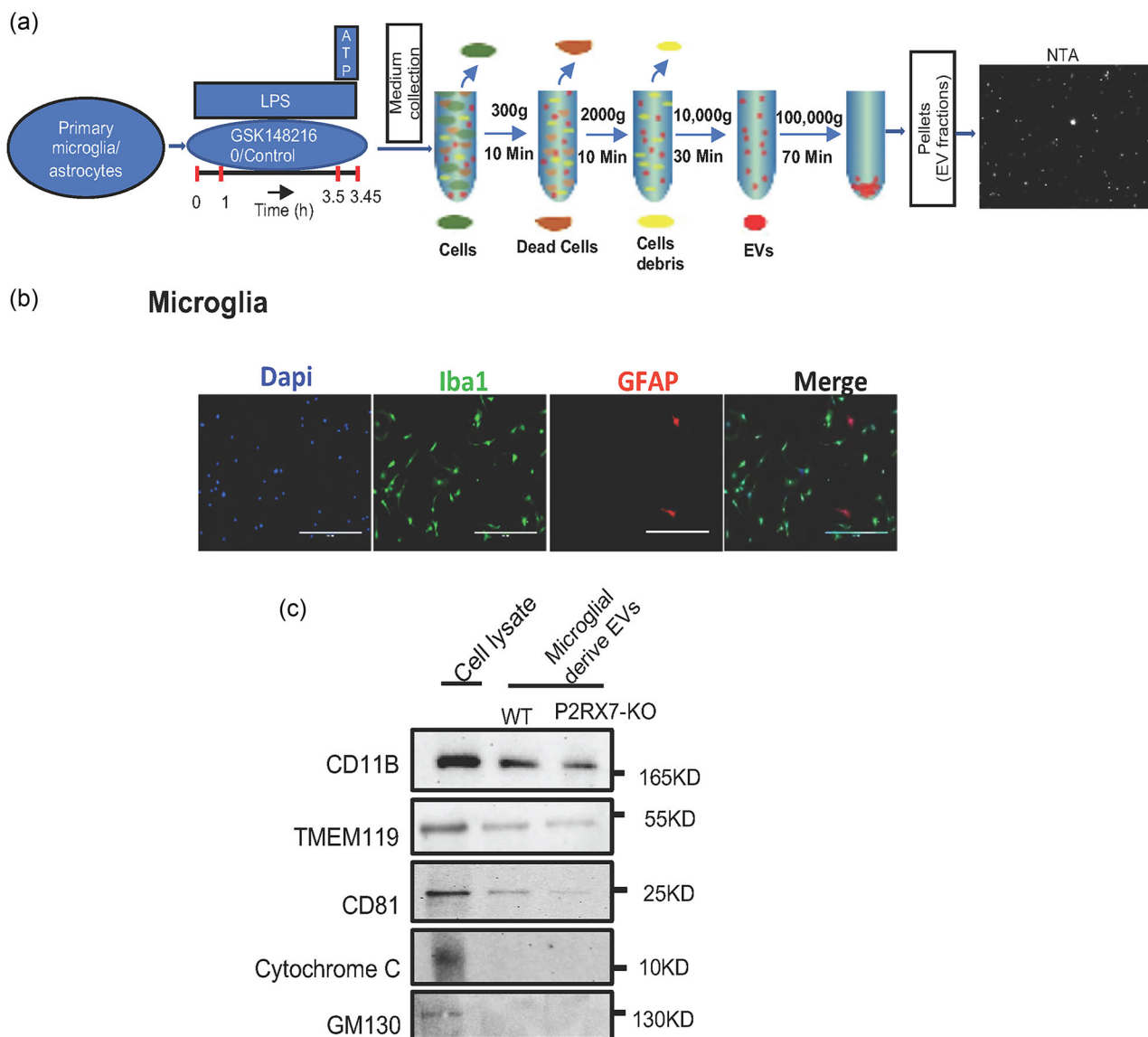


FIGURE 1 Primary culture of microglia and EV isolation. (a) Schematic diagram of the experimental design. (b) Immunocytochemistry of primary cultured microglia by Iba1 (green) and GFAP (red). (c) Western blotting of the WT microglial cell lysate and isolated EVs from and *P2rx7*^{-/-} microglia for CD11B, TMEM119, CD81, Cytochrome C and GM130.

formed by Student's two-tailed unpaired *t*-tests. Multiple comparisons were analyzed by two-way ANOVA, followed by Tukey's multiple comparison test using Prism 10.0 (GraphPad Software). $p < 0.05$ was considered significant

3 | RESULTS

3.1 | Deletion of P2RX7 and GSK1482160 suppresses ATP-induced EV secretion from microglia

To determine the effect of P2RX7 on EV release from primary murine microglia, cells were isolated and cultured from P0-1 WT and *P2rx7*^{-/-} pups, incubated with GSK1482160 or the control for 4 h, primed by LPS for 3 h followed by the stimulation with ATP for 15 min. The CM was collected for isolating EVs via the sequential centrifugation and ultracentrifugation (Figure 1a). The purity of microglia was assessed by staining with the Iba1/microglia antibody (Figure 1b), which positivity was detected with more than 95% of cells. There is no difference in the purity of microglia between WT and *P2rx7*^{-/-} group (data not shown). We observed immunoreactivity to microglial markers (CD11B and TMEM119) and EV marker (CD81) with both samples of the cell lysate from WT microglia and EVs from WT and *P2rx7*^{-/-} microglia whereas non-EV markers (Cytochrome C and GM130) were detected only with the cell lysate sample indicating the successful isolation of EVs from microglia (Figure 1c).

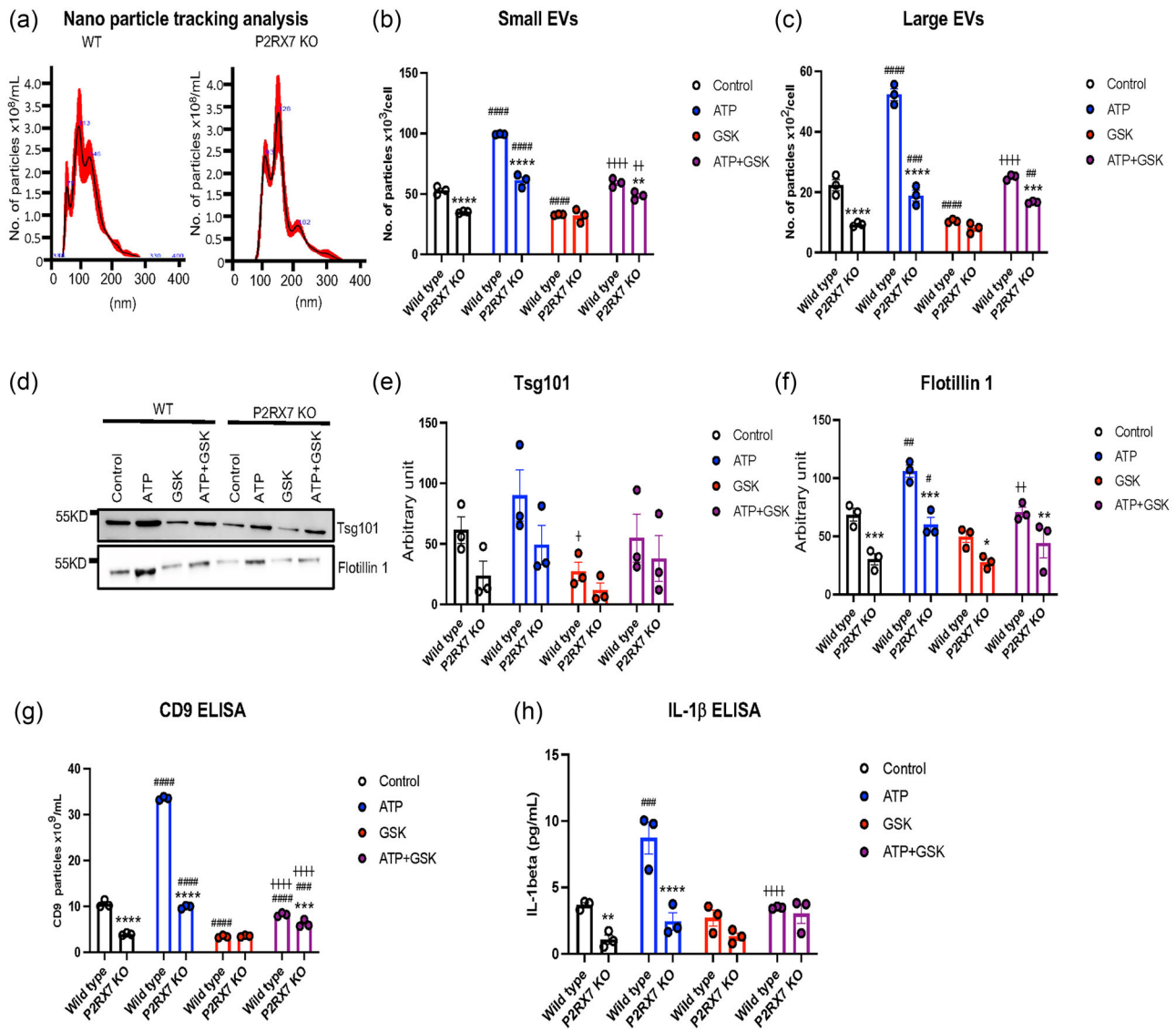


FIGURE 2 Quantification of microglia derived EVs by NTA, immunoblotting and ELISA. (a) NTA plot of mode size and concentration. (b and c) Quantification of EV particle numbers by NTA for small EVs (b) and large EVs (c). (d–f) Immunoblotting and semi quantification of Tsg101 and Flotilin 1 in microglia-derived EVs. (g, h) CD9 ELISA (g) and IL-1β ELISA of microglia-derived EVs (h). (b–h) **p* < 0.05, ***p* < 0.01, ****p* < 0.001, *****p* < 0.0001 between WT and KO within the same treatment condition, #*p* < 0.05, ##*p* < 0.01, ###*p* < 0.001, ####*p* < 0.0001 between control and treated condition of the same genotype group, †*p* < 0.05, ††*p* < 0.01, †††*p* < 0.001, ††††*p* < 0.0001 between ATP and ATP+GSK of the same genotype group as determined by two-way ANOVA followed by Tukey’s multiple comparison test (*N* = 3 per group). Data are representative of at least three independent experiments. Graphs indicate mean ± s.e.m. NTA, nanoparticle tracking analysis.

We next evaluated the effect of GSK1482160 on the secretion of EVs from WT and *P2rx7*^{-/-} microglia by NTA. GSK1482160 was tested at 50 and 100 μM to optimize the dose level. GSK1482160 at 50 and 100 μM equally reduced small and large EV production (Figure S1A–C), hence we used 50 μM for further studies. We separated small EVs (30–150 nm) and large EVs (150–1000 nm) to quantify the number of EVs in each group by NTA (Figure 2a–c). ATP stimulation of microglia significantly increased the number of small and large EVs secreted from WT and *P2rx7*^{-/-} microglia, while deletion of P2RX7 significantly suppressed those numbers at both baseline and ATP-stimulated condition as compared to WT group (Figure 2b,c). GSK1482160 pretreatment significantly reduced ATP-induced secretion of small and large EVs from WT microglia whereas it had no effect on *P2rx7*^{-/-} microglia (Figure 2b,c), suggesting that the effect of GSK1482160 on EV secretion was primarily mediated via P2RX7. These findings were validated by immunoblotting results of EV specific markers, Tsg101 and Flotilin 1 with isolated EVs. The immunoreactivity of Tsg101 in microglia-derived EV was unchanged by the deletion of P2RX7, ATP stimulation or GSK1482160 treatment (Figure 2d,e). Flotilin 1 level, however, was significantly reduced in *P2rx7*^{-/-} microglia-derived EVs compared to WT microglia-derived EVs at both baseline and ATP-stimulated conditions (Figure 2d,f). GSK1482160 treatment diminished the increased level of Flotilin 1 in WT microglia-derived EVs under ATP-stimulated condition, whereas it had no effect on in *P2rx7*^{-/-} microglia-

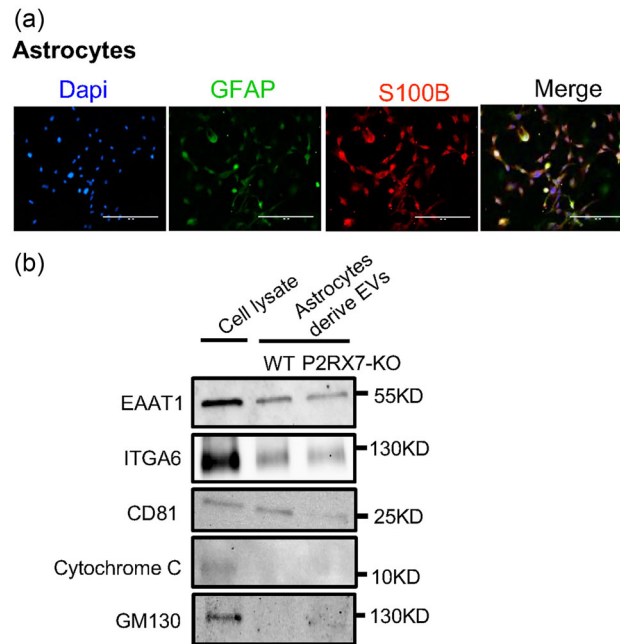


FIGURE 3 Primary culture of astrocytes and EV isolation. (a) Immunocytochemistry of primary cultured astrocytes by GFAP (green) and S100B (red). (b) Western blotting of the WT astrocyte cell lysate and isolated EVs from WT and *P2rx7^{-/-}* astrocytes for EAAT1, ITGA6, CD81, Cytochrome C and GM130.

derived EVs under ATP-stimulated condition (Figure 2f). The SWIFT membrane staining validated the total protein amount used for immunoblotting experiments across all the samples, which showed no significant difference among groups (Figure S2A–D). We further quantified another EV-specific marker, CD9 in EV fractions by ELISA. The results show strong induction of CD9⁺ EV by ATP stimulation in WT microglia, which is significantly blunted in *P2rx7^{-/-}* microglia, and treatment with GSK1482160 significantly suppressed the ATP-induced CD9⁺ EV secretion from both WT and *P2rx7^{-/-}* microglia (Figure 2g). Our group and others previously showed that deletion or inhibition of P2RX7 decreases AD-related pathology in a mouse model whereas P2RX7 activation induces microglial activation and cytokine release (Monif et al., 2009; Ruan et al., 2020; Sanz et al., 2009; Solle et al., 2001). ELISA measurement of IL-1 β showed that deletion of P2RX7 suppressed the baseline and ATP-induced IL-1 β secretion, which was sensitive to the treatment of GSK1482160 in WT microglia but not in *P2rx7^{-/-}* microglia (Figure 2h).

Taken together, these data clearly demonstrate that (1) P2RX7 plays a significant role on baseline and ATP-induced EV secretion from microglia, (2) P2RX7 is responsible for the suppressive effect of GSK1482160 on ATP-induced EV secretion from microglia and (3) P2RX7 is also responsible for ATP-induced IL-1 β secretion from microglia, which is suppressed by GSK1482160 in P2RX7-dependent manner.

3.2 | Deletion of P2RX7 and GSK1482160 suppress ATP-induced EV secretion from astrocytes

We next conducted a similar study using primary murine astrocytes from WT and P2RX7^{-/-} pups. The cell purity was verified by immunostaining of astrocytic markers GFAP and S100B (Figure 3a). There is no difference in the purity of astrocytes between WT and *P2rx7^{-/-}* group (data not shown). Astrocyte-derived EVs were isolated from the CM as shown in Figure 1a. Immunoblotting of the cell lysate from WT astrocytes and EVs derived from WT and *P2rx7^{-/-}* astrocytes show presence of astrocytic EV markers (EAAT1 and ITGA6) (You et al., 2022) and CD81 but EV samples were devoid of non-EVs markers (Cytochrome C and GM130) (Figure 3b). These data show successful tissue culture of astrocytes and enrichment of EVs from the CM.

We next evaluated the effect of deletion of P2RX7 and GSK1482160 treatment for the secretion of ATP-induced EVs from primary cultured astrocytes by NTA. The results are similar to the findings obtained from microglia. ATP stimulation enhanced small or large EV secretion from both WT and *P2rx7^{-/-}* astrocytes, although we observed significant reduction in secretion of small and large EVs from *P2rx7^{-/-}* astrocytes compared to WT group in ATP stimulated conditions (Figure 4a–c). The secretion of small EV was also suppressed in *P2rx7^{-/-}* astrocytes compared to WT astrocytes (Figure 4b). Additionally, GSK1482160 pre-treatment significantly reduced ATP-induced secretion of both small and large EVs from WT astrocytes but not from *P2rx7^{-/-}* astrocytes (Figure 4b,c). The immunoblotting of astrocyte-derived EVs for Tsg101 show no changes at baseline, by ATP stimulation or by GSK1482160 treatment between WT and *P2rx7^{-/-}* group (Figure 4e). Flotilin 1 level, however, shows significant increase after ATP stimulation of WT astrocytes (Figure 4f). Stimulation of *P2rx7^{-/-}* astrocytes by ATP did not significantly

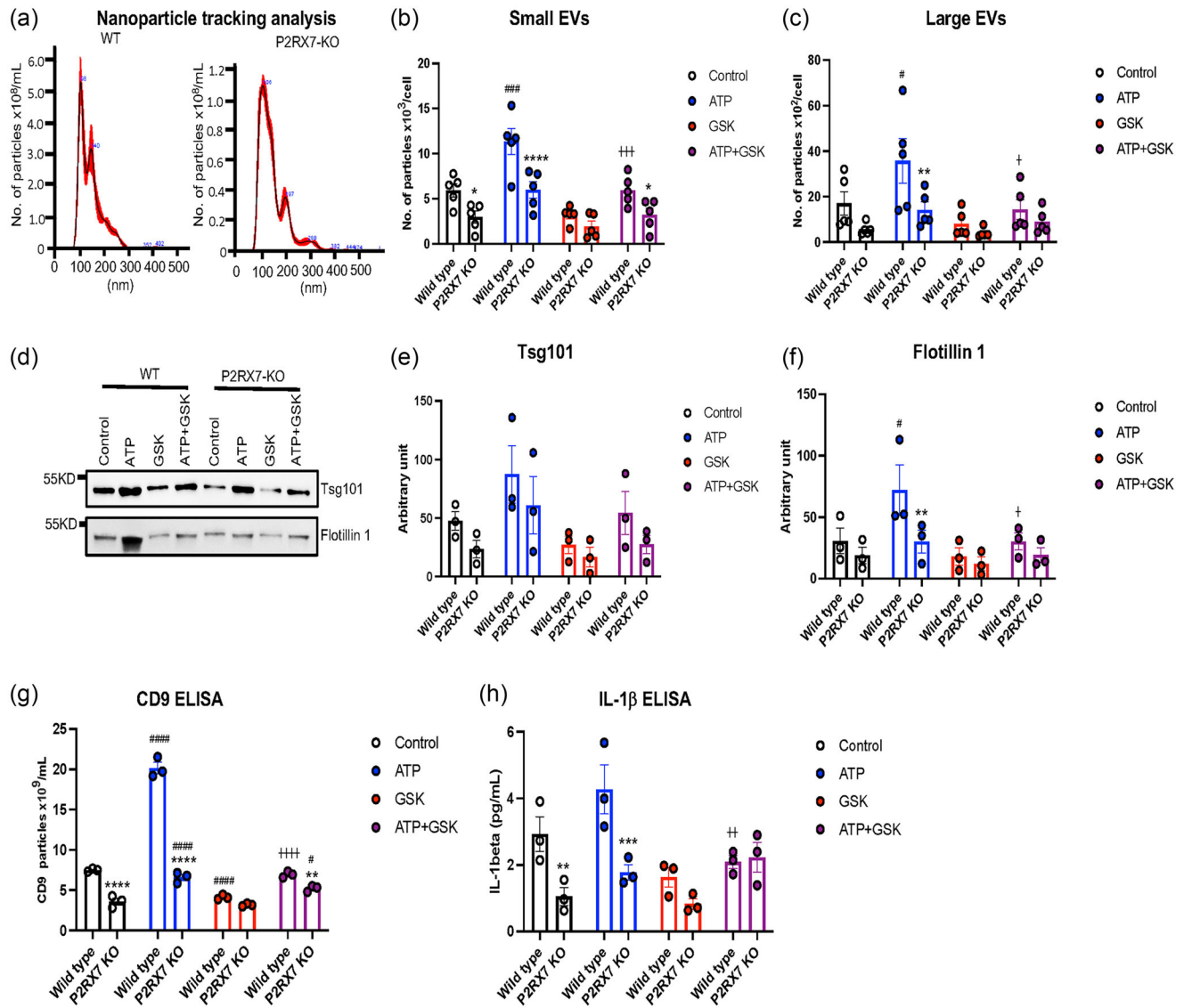


FIGURE 4 Quantification of astrocyte derived EVs by NTA, immunoblotting and ELISA. (a) NTA plot of mode size and concentration (b–c) Quantification of EV particle numbers by NTA for small EVs (b) and large EVs (c). (d–f), Immunoblotting and semi quantification of Tsg101 and Flotilin 1 in astrocyte-derived EVs. (g) CD9 ELISA and (h) IL-1β ELISA of astrocyte-derived EVs. (b–h) * $p < 0.05$, ** $p < 0.01$, *** $p < 0.001$, **** $p < 0.0001$ between WT and KO within the same treatment condition, # $p < 0.05$, ## $p < 0.01$, ### $p < 0.001$, #### $p < 0.0001$ between control and treated condition of the same genotype group, + $p < 0.05$, ++ $p < 0.01$, +++ $p < 0.001$, ++++ $p < 0.0001$ between ATP and ATP+GSK of the same genotype group as determined by two-way ANOVA followed by Tukey’s multiple comparison test ($N = 5$ per group for b–c, $N = 3$ per group for e–h). Data are representative of at least three independent experiments. Graphs indicate mean \pm s.e.m. NTA, nanoparticle tracking analysis.

increase Flotilin-1 immunoreactivity in the EV fraction. Additionally, GSK1482160 treatment significantly suppressed immunoreactivity of Flotilin-1 in the EV fraction from WT astrocyte-derived EVs after ATP stimulation while no significant changes were observed in *P2rx7*^{-/-} group. SWIFT membrane staining was used to detect total protein for immunoblotting experiments which were not significantly different among groups (Figure S3A–D). Quantification of CD9 in the EVs by ELISA shows that (1) Secretion of CD9⁺ EV was significantly reduced at baseline in *P2rx7*^{-/-} astrocytes, (2) ATP significantly stimulated secretion of CD9⁺ EV from both WT and *P2rx7*^{-/-} astrocytes, although it was significantly suppressed in *P2rx7*^{-/-} astrocytes and (3) GSK1482160 pretreatment completely suppressed ATP-induced secretion of CD9⁺ EV from WT astrocytes but not from *P2rx7*^{-/-} astrocytes (Figure 4g). ELISA-based quantification of IL-1β secreted from astrocytes shows that (1) IL-1β secretion was significantly lower from *P2rx7*^{-/-} astrocytes compared to WT group at both baseline and ATP-stimulated conditions, and (2) ATP stimulation failed to increase IL-1β secretion from WT or *P2rx7*^{-/-} astrocytes (Figure 4h). Additionally, GSK1482160 pretreatment significantly suppressed IL-1β secretion from ATP-stimulated WT astrocytes, while it had no effect on *P2rx7*^{-/-} astrocytes. Taken together, these data demonstrate that (1) P2RX7 plays a significant role on baseline and ATP-induced EV secretion from astrocytes, (2) P2RX7 is responsible for the suppressive effect of GSK1482160 on large and CD9⁺ EV secretion from astrocytes and (3) P2RX7 is also responsible for

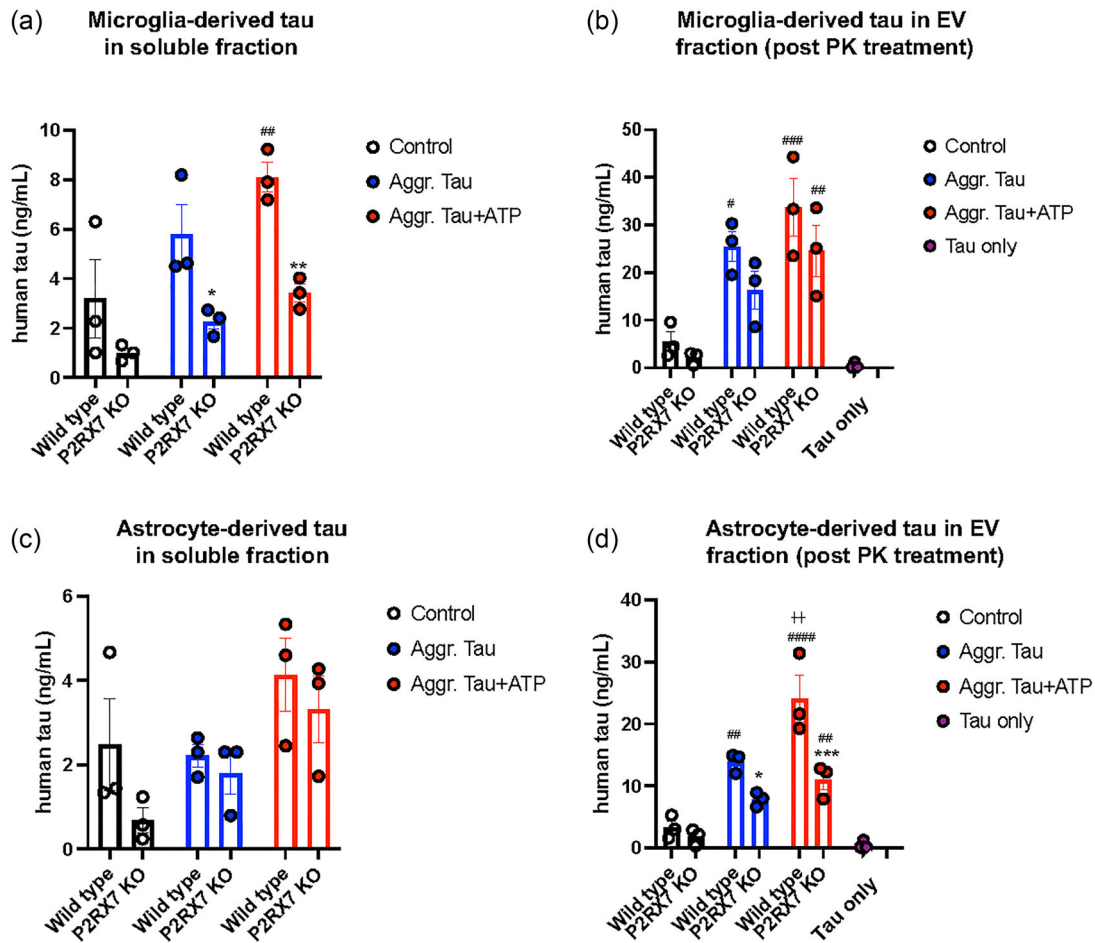


FIGURE 5 Evaluation of soluble and EV-containing hTau aggregates secreted from microglia and astrocytes. EVs were isolated from the culture media of WT or *P2rx7*^{-/-} microglia (a, b) and astrocytes (c, d) after phagocytosis of 10 µg/mL aggregated hTau, followed by ATP stimulation. (a, c) Soluble hTau ELISA, (b, d) hTau ELISA of isolated EVs after proteinase K (PK) treatment. $p < 0.05$, $**p < 0.01$, $***p < 0.001$, $****p < 0.0001$ between WT and KO within the same treatment condition, # $p < 0.05$, ## $p < 0.01$, ### $p < 0.001$, #### $p < 0.0001$ between control and treated condition of the same genotype group as determined by two-way ANOVA followed by Tukey's multiple comparison test ($N = 3$ per group). Data are representative of at least three independent experiments. Graphs indicate mean \pm s.e.m.

IL-1 β secretion from astrocytes at both baseline and ATP-stimulated conditions. We also found that ATP stimulation did not significantly increase IL-1 β secretion from WT or *P2rx7*^{-/-} astrocytes.

3.3 | Microglia and astrocytes secrete tau aggregates in EVs in P2RX7-dependent manner

We have previously shown that GSK1482160 treatment suppress ATP-induced tau secretion in the EVs from microglia (Ruan et al., 2020). We thus evaluated the effect of *P2rx7* deletion on loading of aggregated tau in EVs secreted from WT and *P2rx7*^{-/-} microglia or astrocytes after their uptake of aggregated human tau 1–441 (hTau). For that purpose, primary cultured WT and *P2rx7*^{-/-} microglia and astrocytes were pre-incubated with aggregated hTau for 24 h, stimulated by LPS and ATP to isolate soluble and EV fractions from the CM. To avoid potential contamination of aggregated tau in the EV fraction by centrifugation, we applied qEV-based purification process after the centrifugation and treatment of EVs with proteinase K (PK) to remove tau aggregates attached to the EVs. ATP stimulation significantly enhanced soluble tau secretion from WT but not from *P2rx7*^{-/-} microglia (Figure 5a). We observed 5-fold enrichment of aggregated tau in PK-resistant EV fraction over soluble fraction in both base line and ATP-treated conditions (Figure 5b). The PK-resistant tau level in the EVs were significantly increased by ATP stimulation of WT microglia but not of *P2rx7*^{-/-} microglia (Figure 5b). The effect of PK treatment is sufficient as we observed 99.8% digestion of 0.5 µg soluble tau in the same condition (Figure 5b). In astrocytes: (1) ATP stimulation has no significant effect on secretion of soluble hTau from WT or *P2rx7*^{-/-} astrocytes (Figure 5c), (2) there was 5-fold enrichment of tau in PK-resistant EV fractions over soluble fractions and (3) ATP stimulation significantly increased the level of PK-resistant hTau in EVs from

WT but not from *P2rx7*^{-/-} astrocytes (Figure 5d), (4) EV from *P2rx7*^{-/-} astrocytes has significantly lower level of PK-resistant tau after phagocytosis of aggregated tau with or without ATP stimulation. Taken together, these findings show that not only microglia, but astrocytes also uptake and secrete hTau aggregates in both soluble and EV fractions, which was increased by ATP stimulation in P2RX7-dependent manner.

4 | DISCUSSION

Our study showed that ATP stimulation and P2RX7 regulates EV secretion, IL-1 β secretion and EV-tau secretion from microglia and astrocytes. As we expected, the effect of GSK1482160 on those measures are primarily mediated through inhibition of P2RX7. P2RX7 is highly expressed in microglia in both healthy and diseased brains. In terms of the relevance of P2RX7 in neurodegenerative disorders, *P2rx7* deficiency in tau transgenic mice show reduced number of Iba1⁺ microglia, supporting the idea that P2RX7 also modulates microglial homeostasis (Kaczmarek-Hajek et al., 2018). Recent study by Carvalho et al. revealed that P2RX7 expression was elevated in the brains of FTLD-tau patients and in the hippocampus of transgenic mice that developed tauopathies, supporting the hypothesis that P2RX7 expression is positively correlated with tau pathology (Carvalho et al., 2021). P2RX7 expression is also elevated in the brains of Alzheimer's patients, particularly in microglia and astrocytes around amyloid plaques (Martin et al., 2019; McLarnon et al., 2006). *P2rx7* deficiency also reduced A β load and improved cognitive functions in APP/PS1 mice (Martin et al., 2019). P2RX7 could therefore be a legitimate therapeutic target for halting the progression of tauopathy and A β accumulation in AD.

Although P2RX7 is mainly expressed in microglia in the CNS, it is also detected in oligodendrocytes (Kaczmarek-Hajek et al., 2018) and in activated astrocytes in P301S tau mice (Jin et al., 2018). In this study, we discovered that *P2rx7* deletion impacts EV secretion from not only microglia but also astrocytes in the baseline and ATP stimulated conditions compared to the WT control group as determined by NTA, biochemical assessment of EV markers, IL-1 β secretion and EV-mediated secretion of PK-resistant hTau aggregates.

Our study also suggests that other purinergic receptors are involved in ATP-induced EV secretion, since ATP stimulation still modestly increased secretion of small and large EVs from *P2rx7*^{-/-} microglia and astrocytes, which are insensitive to GSK1482160 treatment except small EV secretion from *P2rx7*^{-/-} astrocytes. Other purinergic receptors, such as P2RX4, are also expressed in microglia and astrocytes (Ashour & Deuchars, 2004; Hua et al., 2023). These additional receptors may also play a role for ATP-induced EV secretion from glia.

In conclusion, our study showed decreased EV secretion from primary cultured *P2rx7*^{-/-} microglia and astrocytes compared to the WT group in both baseline and the ATP-stimulated conditions. Furthermore, pretreatment of cells with GSK1482160 had a significant impact on EV secretion from WT astrocytes and microglia, which was diminished in *P2rx7*^{-/-} group. The study demonstrate that P2RX7 is an important molecule for ATP-induced secretion of EVs, IL-1 β and EV-tau in microglia and astrocytes, further corroborating an idea that targeting P2RX7 in AD and related tauopathies could be a promising therapeutic approach.

AUTHOR CONTRIBUTIONS

Tsuneya Ikezu; Seiko Ikezu and Mohammad Abdullah designed the research; **Tsuneya Ikezu; Zhi Ruan and Seiko Ikezu** provided the oversight and suggestion on data interpretation; **Mohammad Abdullah** performed the experiments and wrote the manuscript. **Tsuneya Ikezu and Seiko Ikezu** assisted with the manuscript writing and editing. **Tsuneya Ikezu** supervised the study and contributed to manuscript preparation and editing. All authors have read and approved the final version of the manuscript. All authors have no conflict of interest in this study.

ACKNOWLEDGEMENTS

We would like to thank the other members of the Molecular Neurotherapeutics Laboratory at Mayo Clinic Florida. This work is funded in part by Cure Alzheimer's Fund (TI, SI), NIH RFI AG054199 (TI), R01AG054672, R01 AG066429 (TI), R01 AG067763 (TI), R01 AG072719 (TI), RFI AG082704 (TI, SI) and R01 AG079859 (SI).

CONFLICT OF INTEREST STATEMENT

The authors declare no conflicts of interest

ORCID

Tsuneya Ikezu  <https://orcid.org/0000-0002-3979-8596>

REFERENCES

Abdullah, M., Takase, H., Nunome, M., Enomoto, H., Ito, J., Gong, J. S., & Michikawa, M. (2016). Amyloid-beta reduces exosome release from astrocytes by enhancing JNK phosphorylation. *Journal of Alzheimer's Disease*, 53, 1433–1441.

- Asai, H., Ikezu, S., Tsunoda, S., Medalla, M., Luebke, J., Haydar, T., Wolozin, B., Butovsky, O., Kugler, S., & Ikezu, T. (2015). Depletion of microglia and inhibition of exosome synthesis halt tau propagation. *Nature Neuroscience*, *18*, 1584–1593.
- Ashour, F., & Deuchars, J. (2004). Electron microscopic localisation of P2 \times 4 receptor subunit immunoreactivity to pre- and post-synaptic neuronal elements and glial processes in the dorsal vagal complex of the rat. *Brain Research*, *1026*, 44–55.
- Braak, H., & Braak, E. (1991). Neuropathological staging of Alzheimer-related changes. *Acta Neuropathologica*, *82*, 239–259.
- Brier, M. R., Gordon, B., Friedrichsen, K., McCarthy, J., Stern, A., Christensen, J., Owen, C., Aldea, P., Su, Y., Hassenstab, J., Cairns, N. J., Holtzman, D. M., Fagan, A. M., Morris, J. C., Benzinger, T. L., & Ances, B. M. (2016). Tau and A β imaging, CSF measures, and cognition in Alzheimer's disease. *Science Translational Medicine*, *8*, 338ra366.
- Carvalho, K., Martin, E., Ces, A., Sarrazin, N., Lagouge-Roussey, P., Nous, C., Boucherit, L., Youssef, I., Prigent, A., Faivre, E., Eddarkaoui, S., Gauvrit, T., Vieau, D., Boluda, S., Huin, V., Fontaine, B., Buee, L., Delatour, B., Dutar, P., & Neuro, C. E. B. B. (2021). P2 \times 7-deficiency improves plasticity and cognitive abilities in a mouse model of Tauopathy. *Progress in Neurobiology*, *206*, 102139.
- Crotti, A., Sait, H. R., McAvoy, K. M., Estrada, K., Ergun, A., Szak, S., Marsh, G., Jandreski, L., Peterson, M., Reynolds, T. L., Dalkilic-Liddle, I., Cameron, A., Cahir-McFarland, E., & Ransohoff, R. M. (2019). BIN1 favors the spreading of Tau via extracellular vesicles. *Scientific Reports*, *9*, 9477.
- Gong, J. S., Kobayashi, M., Hayashi, H., Zou, K., Sawamura, N., Fujita, S. C., Yanagisawa, K., & Michikawa, M. (2002). Apolipoprotein E (ApoE) isoform-dependent lipid release from astrocytes prepared from human ApoE3 and ApoE4 knock-in mice. *Journal of Biological Chemistry*, *277*, 29919–29926.
- Gu, B. J., Field, J., Dutertre, S., Ou, A., Kilpatrick, T. J., Lechner-Scott, J., Scott, R., Lea, R., Taylor, B. V., Stankovich, J., Butzkueven, H., Gresle, M., Laws, S. M., Petrou, S., Hoffman, S., Akkad, D. A., Graham, C. A., Hawkins, S., Glaser, A., & Wiley, J. S. (2015). A rare P2 \times 7 variant Arg307Gln with absent pore formation function protects against neuroinflammation in multiple sclerosis. *Human Molecular Genetics*, *24*, 5644–5654.
- Hua, J., Garcia de Paco, E., Linck, N., Maurice, T., Desrumaux, C., Manoury, B., Rassendren, F., & Ulmann, L. (2023). Microglial P2 \times 4 receptors promote ApoE degradation and contribute to memory deficits in Alzheimer's disease. *Cellular and Molecular Life Sciences*, *80*, 138.
- Ikezu, S., Yeh, H., Delpech, J. C., Woodbury, M. E., Van Enoo, A. A., Ruan, Z., Sivakumaran, S., You, Y., Holland, C., Guillamon-Vivancos, T., Yoshii-Kitahara, A., Botros, M. B., Madore, C., Chao, P. H., Desani, A., Manimaran, S., Kalavai, S. V., Johnson, W. E., Butovsky, O., & Ikezu, T. (2021). Inhibition of colony stimulating factor 1 receptor corrects maternal inflammation-induced microglial and synaptic dysfunction and behavioral abnormalities. *Molecular Psychiatry*, *26*, 1808–1831.
- Jin, H., Han, J., Resing, D., Liu, H., Yue, X., Miller, R. L., Schoch, K. M., Miller, T. M., Perlmutter, J. S., Egan, T. M., & Tu, Z. (2018). Synthesis and in vitro characterization of a P2 \times 7 radioligand [(123)I]TZ6019 and its response to neuroinflammation in a mouse model of Alzheimer disease. *European Journal of Pharmacology*, *820*, 8–17.
- Kaczmarek-Hajek, K., Zhang, J., Kopp, R., Grosche, A., Rissiek, B., Saul, A., Bruzzone, S., Engel, T., Jooss, T., Krautloher, A., Schuster, S., Magnus, T., Stadelmann, C., Sirko, S., Koch-Nolte, F., Eulenburg, V., & Nicke, A. (2018). Re-evaluation of neuronal P2 \times 7 expression using novel mouse models and a P2 \times 7-specific nanobody. *Life*, *7*, e36217.
- Lebouvier, T., Pasquier, F., & Buee, L. (2017). Update on tauopathies. *Current Opinion in Neurology*, *30*, 589–598.
- Martin, E., Amar, M., Dalle, C., Youssef, I., Boucher, C., Duigou, C. Le, Bruckner, M., Prigent, A., Sazdovitch, V., Halle, A., Kanellopoulos, J. M., Fontaine, B., Delatour, B., & Delarasse, C. (2019). New role of P2 \times 7 receptor in an Alzheimer's disease mouse model. *Molecular Psychiatry*, *24*, 108–125.
- McLarnon, J. G., Ryu, J. K., Walker, D. G., & Choi, H. B. (2006). Upregulated expression of purinergic P2X(7) receptor in Alzheimer disease and amyloid-beta peptide-treated microglia and in peptide-injected rat hippocampus. *Journal of Neuropathology and Experimental Neurology*, *65*, 1090–1097.
- Monif, M., Reid, C. A., Powell, K. L., Smart, M. L., & Williams, D. A. (2009). The P2 \times 7 receptor drives microglial activation and proliferation: a trophic role for P2 \times 7R pore. *Journal of Neuroscience*, *29*, 3781–3791.
- Muraoka, S., DeLeo, A. M., Sethi, M. K., Yukawa-Takamatsu, K., Yang, Z., Ko, J., Hogan, J. D., Ruan, Z., You, Y., Wang, Y., Medalla, M., Ikezu, S., Chen, M., Xia, W., Gorantla, S., Gendelman, H. E., Issadore, D., Zaia, J., & Ikezu, T. (2020). Proteomic and biological profiling of extracellular vesicles from Alzheimer's disease human brain tissues. *Alzheimers Dementia*, *16*, 896–907.
- Ruan, Z., Delpech, J. C., Venkatesan Kalavai, S., Van Enoo, A. A., Hu, J., Ikezu, S., & Ikezu, T. (2020). P2RX7 inhibitor suppresses exosome secretion and disease phenotype in P301S tau transgenic mice. *Molecular Neurodegeneration*, *15*, 47.
- Ruan, Z., Pathak, D., Venkatesan Kalavai, S., Yoshii-Kitahara, A., Muraoka, S., Bhatt, N., Takamatsu-Yukawa, K., Hu, J., Wang, Y., Hersh, S., Ericsson, M., Gorantla, S., Gendelman, H. E., Kaye, R., Ikezu, S., Luebke, J. I., & Ikezu, T. (2021). Alzheimer's disease brain-derived extracellular vesicles spread tau pathology in interneurons. *Brain*, *144*, 288–309.
- Sanz, J. M., Chiozzi, P., Ferrari, D., Colaianna, M., Idzko, M., Falzoni, S., Fellin, R., Trabace, L., & Di Virgilio, F. (2009). Activation of microglia by amyloid beta requires P2 \times 7 receptor expression. *Journal of Immunology*, *182*, 4378–4385.
- Solle, M., Labasi, J., Perregaux, D. G., Stam, E., Petrushova, N., Koller, B. H., Griffiths, R. J., & Gabel, C. A. (2001). Altered cytokine production in mice lacking P2X(7) receptors. *Journal of Biological Chemistry*, *276*, 125–132.
- You, Y., Muraoka, S., Jedrychowski, M. P., Hu, J., McQuade, A. K., Young-Pearse, T., Aslebagh, R., Shaffer, S. A., Gygi, S. P., Blurton-Jones, M., Poon, W. W., & Ikezu, T. (2022). Human neural cell type-specific extracellular vesicle proteome defines disease-related molecules associated with activated astrocytes in Alzheimer's disease brain. *Journal of Extracellular Vesicles*, *11*, e12183.

SUPPORTING INFORMATION

Additional supporting information can be found online in the Supporting Information section at the end of this article.

How to cite this article: Abdullah, M., Ruan, Z., Ikezu, S., & Ikezu, T. (2024). P2RX7 plays a critical role in extracellular vesicle-mediated secretion of pathogenic molecules from microglia and astrocytes. *Journal of Extracellular Biology*, *3*, e155. <https://doi.org/10.1002/jex2.155>